Supplemental Figures for:
eIF2α phosphorylation-dependent translation in CA1 pyramidal cells impairs hippocampal memory consolidation without affecting general translation

Zhihong Jiang[1], Juan E. Belforte[1], Yuan Lu[2], Yoko Yabe[1], James Pickel[3], Carolyn Beebe Smith[4], Hyun-Soo Je[5], Bai Lu[2,5], and Kazu Nakazawa[1]

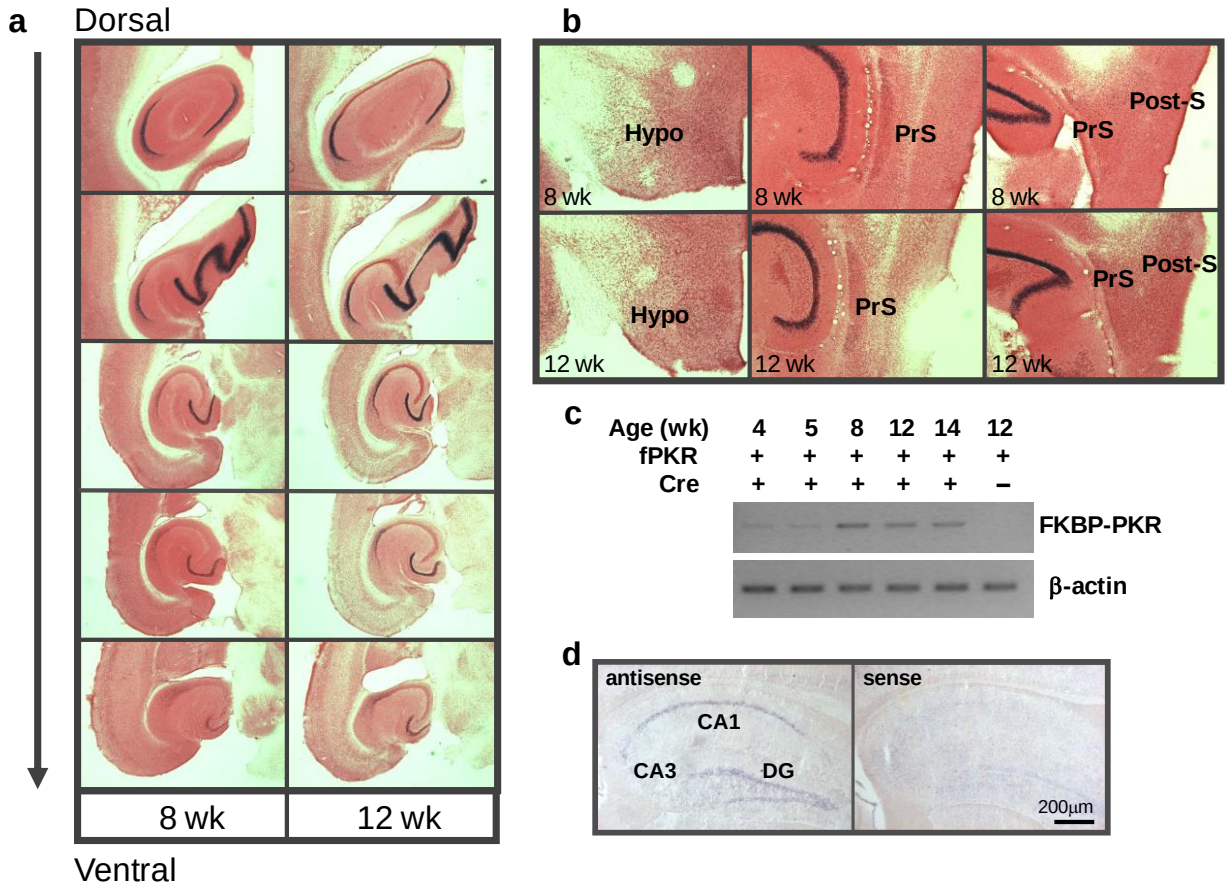

Supplemental Figure 1. (**a**) X-gal staining of a series of horizontal sections along the dorsoventral axis in 8- and 12-week-old fPKR mouse brains revealed that LacZ expression was robust in dorsal CA1 pyramidal cells and dentate granule cells whose expression was declined towards ventral hippocampi. (**b**) LacZ-positive cells in 8- and 12-week-old fPKR mouse brains were sporadically observed in hypothalamic nuclei (coronal sections) and pre- and postsubiculum (parasagittal sections). Hypo, hypothalamus; PrS, presubiculum; Post-S, postsubiculum. (**c**) RT-PCR to detect FKBP-PKR mRNA transcription in mutants. Total RNA was extracted from the hippocampi of mutant mice aged 4 to 14 weeks. RNA from 12-week-old fPKR mice was used as control. (**d**) *In situ* hybridization using human PKR specific RNA probes showed the over-expression of FKBP-PKR in CA1 pyramidal cells and dentate granule cells of the mutants. Sections from 12-week-old mutant mice were incubated with human specific PKR antisense or sense RNA probes.

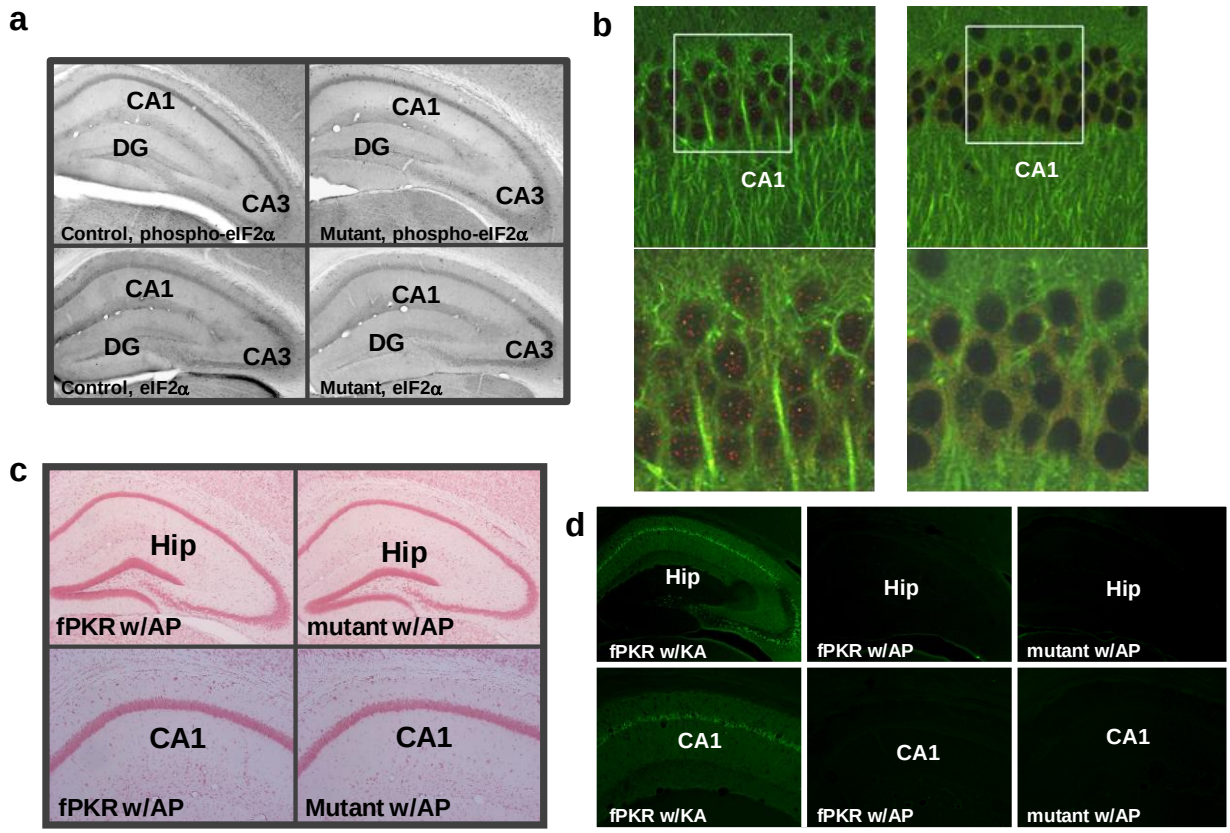

Supplemental Figure 2. (**a**) Expression levels of phospho-eIF2α and eIF2α protein in the dorsal hippocampus from mutants and fPKR controls without AP20187 infusion were examined by immuno-staining with anti-phospho-eIF2α and anti-eIF2α. Compared to CA1 pyramidal cell layers, extremely low levels of phospho-eIF2α and eIF2α protein were observed in dentate granule cell layers in both mutant and fPKR mice. (**b**) Sections from mutant animals 2 hr after AP20187 infusion were double-immunostained with anti-ATF4 (red signal in left panel) and anti-MAP2 (green signal). The red signal for ATF4 was disappeared when ATF4 antibody was incubated with ATF4 blocking peptide (right panel). The images were collected by confocal microscope. The boxed areas from the top panels are enlarged in the bottom panels. (**c**) Twelve-week-old mutants and fPKR control mice were *i.c.v.* injected with AP20187 through infusion cannula, and were sacrificed 24hr later. Coronal brain sections were Nissl-stained with Safranin O. No apparent cell loss or structural abnormality was observed after AP20187 infusion. w/AP, with AP20187. (**d**) Brain sections from mutants and fPKR controls were subjected to Fluoro-Jade B staining to investigate neurodegeneration 24 hr after AP20187 infusion. No staining was observed in sections from fPKR control and mutant mice after treatment with AP20187. Sections from fPKR controls treated with kainic acid (KA, Tocris) *i.c.v.* injection (0.2 μg) exhibited massive neuronal degeneration in hippocampal CA1 and CA3. w/KA, with kainic acid.

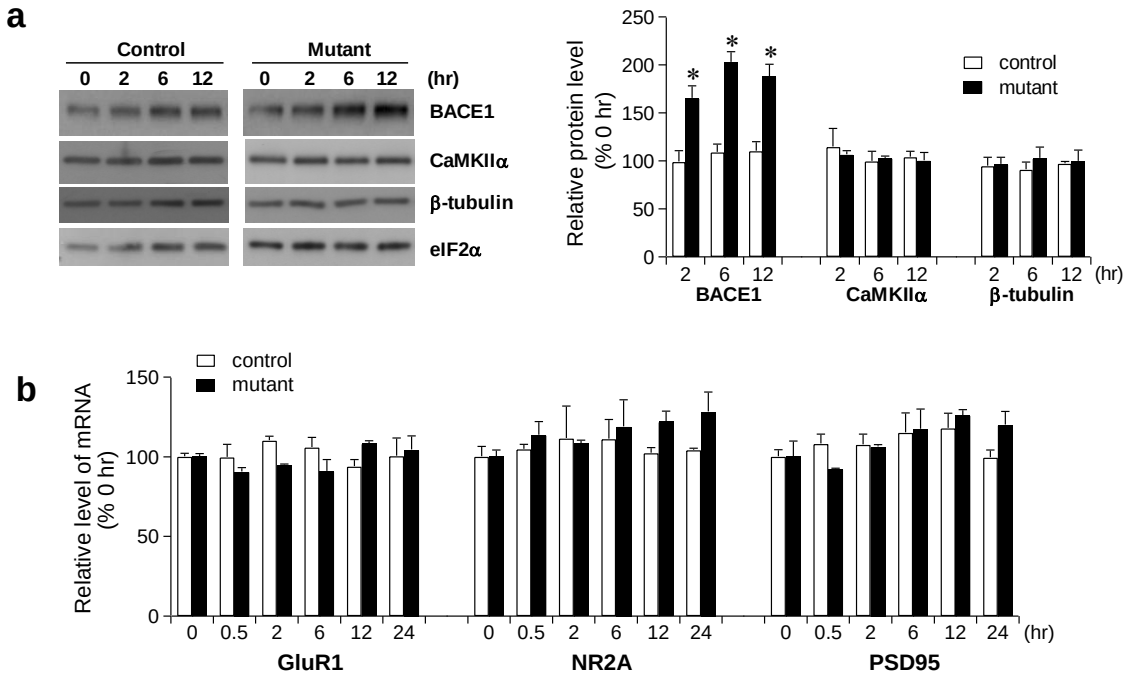

Supplemental Figure 3. (**a**) BACE1 protein levels in the mutant hippocampal CA1 were increased by Western blots following elevation of phospho-eIF2α after AP20187 injection. Protein levels of CaMKIIα and ß-tubulin were not altered. Three animals were used for each group. Total protein loading was normalized by Western blots with anti-eIF2α Ab. Relative protein levels (%) upon AP20187 treatment at different time points were compared to those of zero time points of controls or mutants. For BACE1, $F_{1,12}$=70.0 for genotype effect, p<0.000005. *Post hoc* Fisher's LSD test, *P<0.05. (**b**) Gene transcription of GluR1, NR2A, or PSD95 was not affected after AP20187 injection in mutant hippocampal CA1. Relative mRNA level (%) for each gene at different time points after AP20187 treatment was detected by RT-PCR and compared to those of zero time point of controls or mutants. PCR products were normalized by GAPDH transcripts. *Post hoc* Fisher's LSD test, P>0.05 for any time point between genotypes.

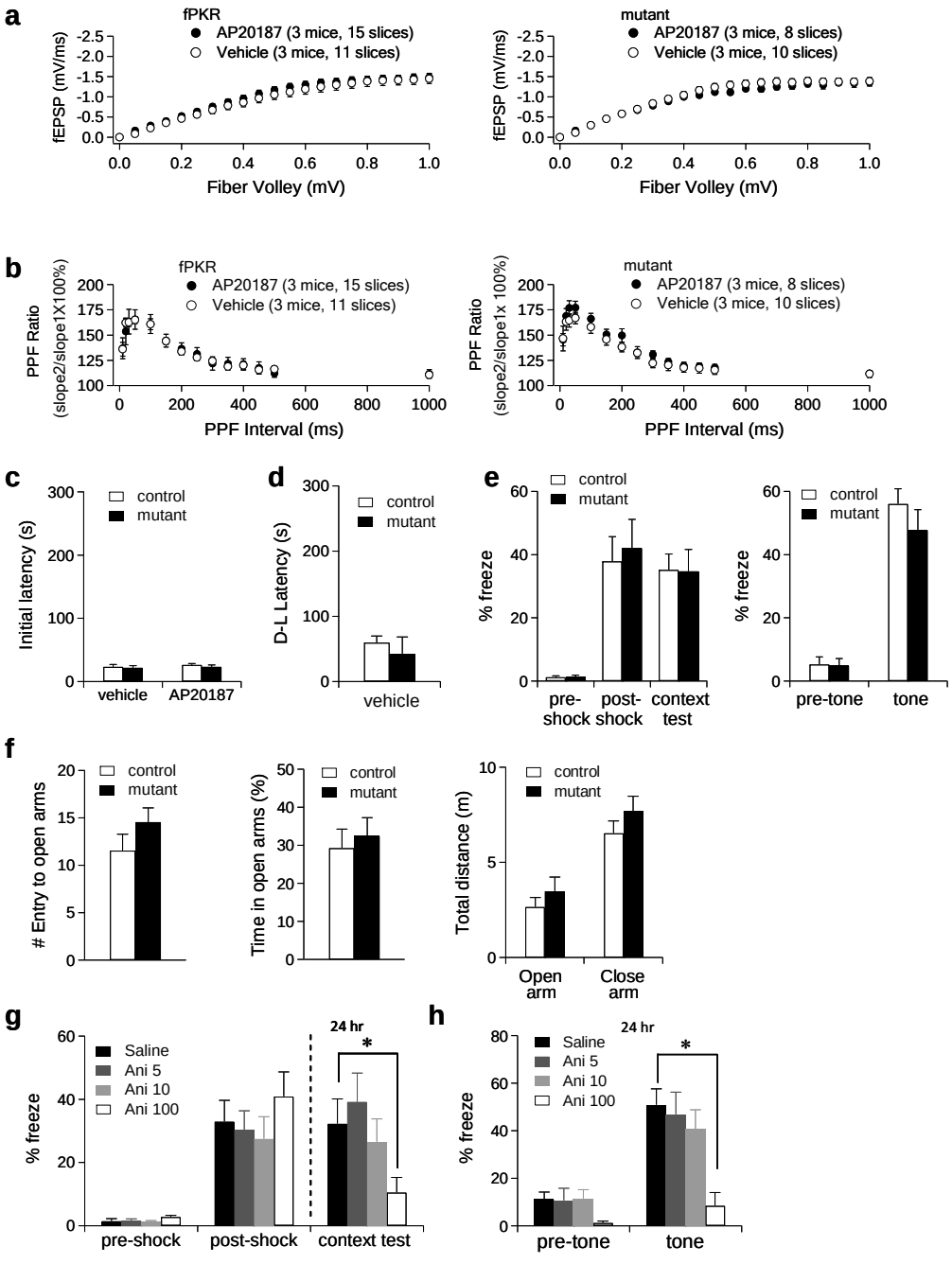

Supplemental Figure 4. (**a**) Input-output curves with the postsynaptic response (initial slope of fEPSP) plotted as a function of the presynaptic fiber volley amplitude, were indistinguishable between AP20187 (filled circle) and vehicle control (open circle) for each genotype. (**b**) In the hippocampal slice recording, paired pulse facilitation was virtually identical for AP20187 (filled circle) and vehicle control (open circle) for each genotype over the whole range of interstimulus intervals. (**c**) In step-through active avoidance task, control and mutant mice had similar initial cross latencies from the light to dark compartment of the chamber after injection of saline

vehicle (n=11 for each group) or AP20187 (n=20 for each group). (**d**) Control and mutant animals injected with vehicle 2 hr before training showed the similar short latencies to cross from the dark compartment A to light compartment when tested 24 hr later. N=11 for each group. (**e**) Control and mutant mice with vehicle injection exhibited similar associative memory for context (left panel) and tone (right panel) after a retention delay of 24 hr. N=9 for each group. (**f**) No differences in anxiety or locomotor activity were observed between the genotypes upon AP20187 injection in the elevated plus maze test. N=9 for each group. (**g**-**h**) Mice were subjected to fear conditioning and contextual freezing immediately after footshock was similar among groups (**g**). However, 24 hr after training, Contextual (**g**) and cued-fear memory (**h**) were impaired with injection of 100 mg/kg anisomycin but were not impaired with 5 mg/kg or 10 mg/kg of anisomycin immediately after training. N=8 for each groups. One-way ANOVA, post hoc Dunnett test, *P<0.05. Ani 5, anisomycin 5mg/kg; Ani 10, anisomycin 10mg/kg; Ani 100, anisomycin 100mg/kg.